Edge Pedestal Control in Quiescent H-Mode Discharges in DIII-D Using Co Plus Counter Neutral Beam Injection

K.H. Burrell 1), T.H. Osborne 1), P.B. Snyder 1), W.P. West 1), M.S. Chu 1), M.E. Fenstermacher 2), P. Gohil 1), W.M. Solomon 3)

1) General Atomics, P.O. Box 85608, San Diego, California 92186-5608, USA
2) Lawrence Livermore National Laboratory, Livermore, California 94550, USA
3) Princeton Plasma Physics Laboratory, Princeton, New Jersey 08543, USA

e-mail contact of main author: burrell@fusion.gat.com

Abstract. We have made two significant discoveries in our recent studies of quiescent H-mode (QH-mode) plasmas in DIII-D. First, we have found that we can control the edge pedestal density and pressure by altering the edge particle transport through changes in the edge toroidal rotation. This allows us to adjust the edge operating point to be close to, but below the ELM stability boundary, maintaining the ELM-free state while allowing up to a factor of two increase in edge pressure. The ELM boundary is significantly higher in more strongly shaped plasmas, which broadens the operating space available for QH-mode and leads to improved core performance. Second, for the first time on any tokamak, we have created QH-mode plasmas with strong edge co-rotation; previous QH-modes in all tokamaks had edge counter rotation. This result demonstrates that counter NBI and edge counter rotation are not essential conditions for QH-mode. Both these investigations benefited from the edge stability predictions based on peeling-ballooning mode theory. The broadening of the ELM-stable region with plasma shaping is predicted by that theory. The theory has also been extended to provide a model for the edge harmonic oscillation (EHO) that regulates edge transport in the QH-mode. Many of the features of that theory agree with the experimental results reported either previously or in the present paper. One notable example is the prediction that co-rotating QH-mode is possible provided sufficient shear in the edge rotation can be created.

1. Introduction

Quiescent H-mode (QH-mode) plasmas in DIII-D with co plus counter neutral beam injection have demonstrated active control of the edge pedestal that can be used to optimize the edge conditions in future burning plasma devices such as ITER. Burning plasmas impose significant, conflicting constraints on the edge pedestal. To maximize fusion power, H-mode operation is preferred, with an edge pedestal pressure which is as high as possible. However, to eliminate damage to divertor components caused by impulsive heat loads due to edge localized modes (ELMs), ELMs must be eliminated by limiting the edge pressure to a value below that set by the peeling-ballooning mode stability limit. In addition, density control and helium ash removal demand sufficient edge particle transport; ELM-induced particle transport could provide this were it not for the impulsive heat load problem. ELM-free QH-mode plasmas have demonstrated that all these requirements can be met simultaneously in discharges which operate with constant density and radiated power [1]. An example of long pulse, ELM-free QH-mode operation is shown in Fig. 1.

QH-mode was originally discovered on DIII-D [2,3] and was subsequently investigated on ASDEX-Upgrade [4,5], JT-60U [6,7] and JET [5]. QH-modes in DIII-D have been run for long duration, a bit longer than 4 s, which is about 30 energy confinement times, τ_E, or about 2 current relaxation times τ_R [1]. The maximum duration to date has been limited by neutral beam pulse length. Once sufficient power is supplied to create QH-mode (typically 3 to 4 MW), the plasmas remain quiescent even at the input powers needed to reach the core beta limit (typically 15 MW). In addition, the QH-mode edge is quite compatible with core transport barriers; indeed, most QH-mode discharges in DIII-D are quiescent double barrier plasmas with both a core and an edge transport barrier. These plasmas exhibit time-averaged edge particle transport more rapid than that produced by ELMs while operating at reactor relevant pedestal beta ($\beta^{ped} \sim 1\%$) and collisionality ($\nu_i^* = 0.1$) [1,8].

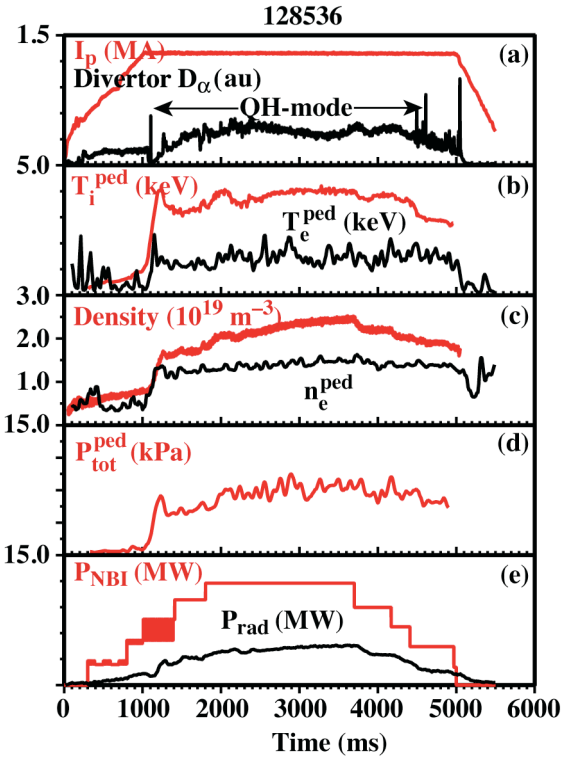

FIG. 1. Time history of long pulse QH-mode. (a) Plasma current and divertor D_α signal, (b) pedestal electron and ion temperature, (c) line averaged and pedestal density, (d) total pedestal pressure, (e) neutral beam input power and total radiated power. Note the complete absence of ELMs during the high power NBI phase.

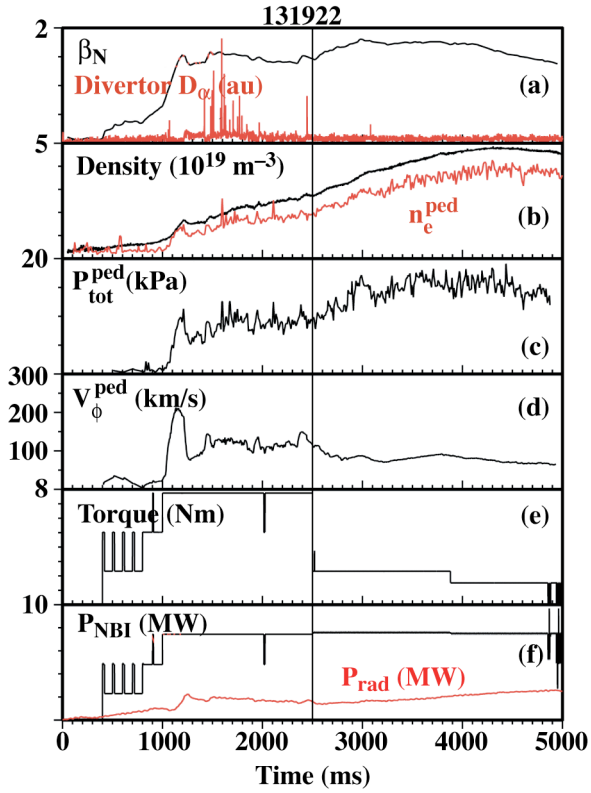

FIG. 2. Time history of QH-mode shot showing increase in stored energy (β_N), pedestal density and pedestal pressure as input torque and edge rotation are reduced. (a) Normalized beta and divertor D_α signal, (b) line averaged and pedestal density, (c) total pedestal pressure, (d) pedestal toroidal rotation speed, (e) NBI input torque, (f) NBI input power and total radiated power. For the direction of the plasma current used here, positive rotation values in (d) and positive torque values in (e) are in the counter direction.

Previous QH-mode plasmas on DIII-D and other devices were usually run with all neutral beam injection (NBI) opposite to the plasma current (counter-injection); this gives input torque and edge pedestal rotation in the counter direction. A major goal of experiments on DIII-D in the last few years was to broaden the QH-mode operating space by exploring QH-mode over a range of input torques, from counter NBI through balanced NBI to all co-NBI.

We have achieved QH-mode operation over a continuous range of input torque from all counter-injection to near balanced injection. As is illustrated in Fig. 2, experiments show that altering the torque input to QH-mode plasmas allows continuous adjustment of the pedestal density, pressure and particle transport over a range of about a factor of 2 while maintaining the ELM-free state. This active control capability allows operation near but below the ELM stability boundary with pedestal densities up to about one-half the Greenwald density [9]. In addition, as is shown in Fig. 3, we have now achieved QH-mode operation with all co-injection in discharges exhibiting rapid co-rotation in the edge pedestal region. Previous experiments on JT-60U which produced QH-mode with net co-injection actually exhibited counter-rotation in the edge pedestal region, possibly due to edge ion loss caused by toroidal field ripple [6,7].

2. Peeling-ballooning Mode Stability and QH-mode Operation

The theory of the stability of the edge peeling-ballooning (kink) modes, embodied for example in the ELITE code [10,11], allowed us to understand a number of features of the QH-mode [12], especially the improvement in QH-mode operating space with plasma shape. This theory has recently been extended to provide a semi-quantitative theory of the edge harmonic oscillation (EHO) [13]. The EHO is an electromagnetic mode localized in the edge pedestal region which provides the extra particle transport necessary to keep the edge operating point below the peeling-ballooning boundary in QH-mode [1,12]. Based on the observation that the predicted growth rates for modes with low toroidal mode number n increase with increasing shear in the edge rotation [13], the theory predicts that the EHO is a low n peeling mode driven unstable by rotational shear at edge conditions slightly below the ELM stability limit in the absence of rotation. As the mode grows to finite amplitude, its magnetic fields interact with the vacuum vessel wall, slowing the plasma rotation, decreasing the rotational shear and, hence, reducing the drive for the mode, thus allowing the mode to saturate at finite amplitude. Experimentally, we see a decrease in edge rotation and an increase in edge particle transport whenever the EHO starts and grows to finite amplitude [1]. The increased particle transport leads to reduced edge density and edge density gradient, which in turn reduces the edge bootstrap current. The reduction in edge pressure gradient and edge current density also reduce the drive for the mode, allowing the plasmas to reach a steady state in the presence of a finite amplitude mode. A more complete theory, however, is still needed to explain how the EHO enhances the edge particle transport. The transport increase is the essential feature that holds the edge pressure gradient and, hence, the edge bootstrap current below the ELM stability limit.

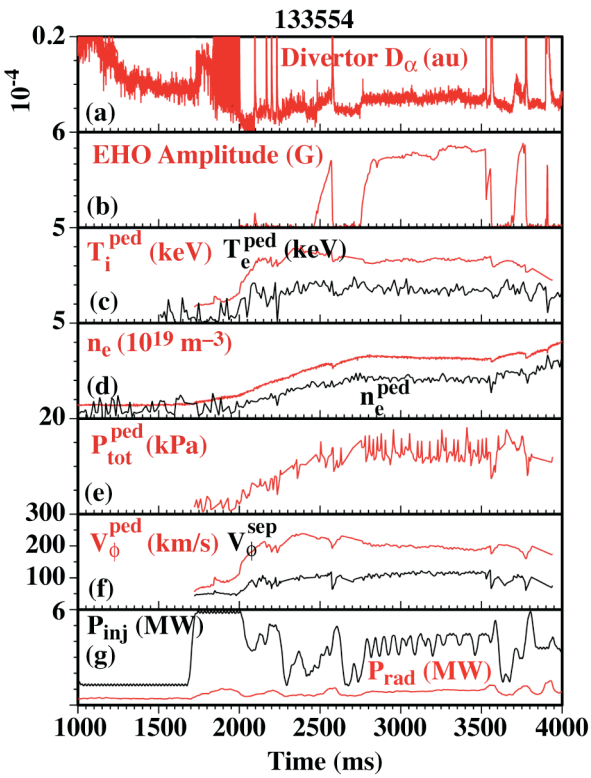

FIG. 3. Time history of QH-mode shot with strong co-rotation. (a) Divertor D_α emission, (b) amplitude of oscillating magnetic field associated with EHO, (c) pedestal electron and ion temperature, (d) line averaged and pedestal electron density, (e) total pedestal pressure, (f) pedestal and separatrix toroidal rotation, (g) NBI input power and total radiated power. For the direction of the plasma current used for this shot, positive rotation values in (f) are in the co-direction. Scale in (a) is chosen so that the increase in the D_α when the EHO turns on can be seen; this demonstrates the increase in particle transport caused by the EHO. Peak ELM amplitude is ~20 times the maximum scale used in (a).

As is illustrated in Fig. 4, the QH-mode operating point is near the peeling stability boundary; this result has been seen for all cases where the edge stability has been analyzed with ELITE [1,8,12,13]. The theory predicts that the EHO should exist near this boundary because the low n modes are the most unstable along this boundary and these are the modes which are further destabilized by rotational shear [13]. The operating point in the stability diagram thus agrees with the experimental observation that QH-modes are produced most easily at low pedestal densities and that the EHO typically has dominant n values in the range of 1 to 3. In addition, because edge stability improves with plasma shaping, especially edge triangularity, the theory predicts a wider operating space for more strongly shaped plasmas,

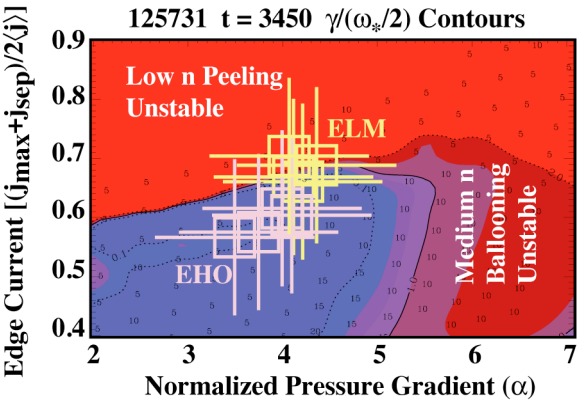

FIG. 4. Peeling-ballooning mode stability diagram showing contours of growth rate of the most unstable mode, γ, divided by one-half the ion diamagnetic frequency, ω^*, plotted as a function of normalized edge pressure gradient and normalized edge current density. Blue regions are stable, red are unstable. The most unstable toroidal mode number increases as the operating point moves from the peeling towards the ballooning boundary. Data points show the operating points for a series of discharges, shots 125729-734, where the edge conditions are changed by changing the edge rotation speed. Note that the QH-mode points with the EHO are further from the stability boundary than the ELMing points.

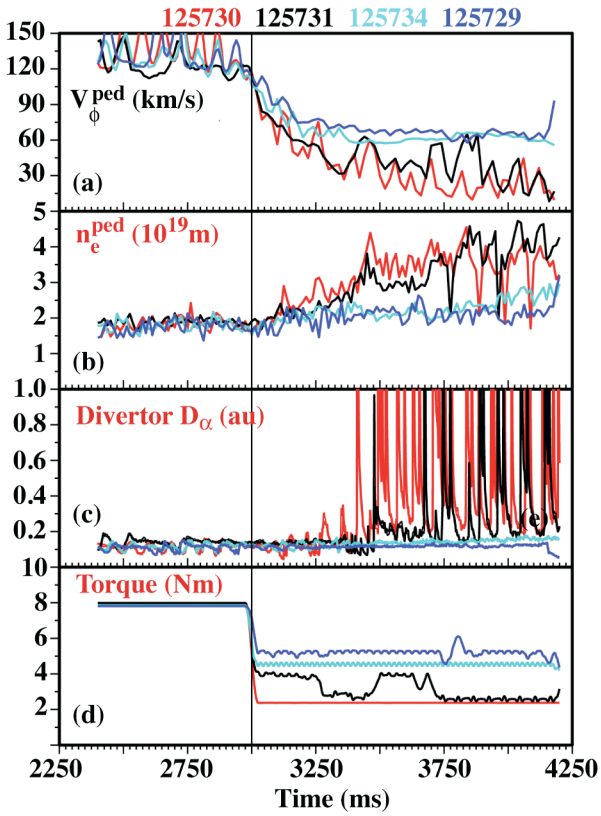

FIG. 5. Variation of (a) pedestal toroidal rotation speed, (b) pedestal density, (c) divertor D_α emission and (d) input torque as a function of time in a sequence of shots where the input torque is systematically varied from shot to shot while keeping the input power essentially constant. As the input torque is reduced, pedestal density increases and the ELMs return. Shots were all QH-mode prior to the change in input torque. In (c), the scale was chosen to allow the baseline to be seen; accordingly, the peak amplitude of the ELMs cannot be seen. It is roughly ten times the full scale value.

with access to the peeling boundary at higher pedestal densities and pressures. Experimentally, higher pedestal densities and pressures can be achieved in QH-modes in more strongly shaped plasmas [1]; this is discussed further in the next section. Finally, the dependence on rotation shear leads to the prediction that QH-mode should be possible with co-NBI provided that sufficient edge rotation shear can be achieved. Experimental results discussed in section 4 now confirm this prediction.

3. QH-mode Operation with Varying NBI Torque

In 2005–2006, one of the neutral beamlines on DIII-D was reoriented so that it injects in the opposite direction to the other three [14]. This allows investigation of the QH-mode behavior as the input torque from NBI is varied while keeping the input power constant. Power variations are known to affect the edge pressure and this technique allows us to eliminate the effects of power variation.

As is shown in Fig. 5, reduction of the input torque leads to a decrease in the pedestal rotation and an increase in the pedestal density. If the density rises too high, the ELMs return; this return of ELMs with increasing density is a common observation in QH-mode. As is demonstrated in Fig. 4, this return of ELMs is consistent with stability calculations using the ELITE code. The ELMing points are systematically closer to the stability boundary than the QH-mode points with the EHO because the edge pressure gradient and, hence, calculated edge bootstrap current have increased.

The increase in pedestal density at constant fueling indicates a decrease in edge particle transport, which is apparently caused by the change in torque or edge rotation. Since the EHO provides the extra particle transport which allows quiescent operation, we speculate that the EHO-induced particle transport is a function of edge rotation speed or edge rotation shear.

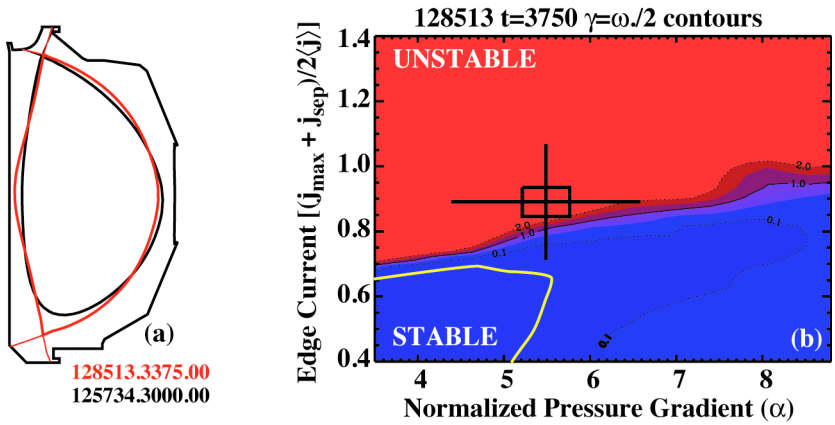

Fig. 6 (a) Comparisons of separatrix shape for the upper single null plasmas used for the results shown in Figs. 4 and 5 (black) compared with the double null divertor plasmas used for results shown in Fig. 2 (red). (b) ELITE stability plot for double-null plasma (128513); the yellow outline is the stability boundary for the single null plasmas. Within the error bar, the operating point for the double null discharge shown in (b) is on the stability boundary.

By utilizing the broader region of edge stability predicted for more highly shaped plasmas [13], we can exploit the sensitivity of the edge transport to rotation to create QH-mode plasmas which remain ELM-free at higher pedestal densities. Figure 6(a) shows the difference in the plasma shape between upper single-null divertor discharges used for the results shown in Figs. 4 and 5 and the double-null discharge used to produce the results shown in Fig. 2. The double-null shape was chosen based on extensive edge stability analysis of a variety of DIII-D discharges [15]. Although the input torque after 2500 ms in Fig. 2 is a factor 1.6 smaller than the lowest torque shown in Fig. 5, the plasma remains in QH-mode with no ELMs. Figure 6(b) compares the edge stability of the single- and double-null discharges, also showing the operating point for one of the double-null discharges. The stable operating space for the double-null plasmas is considerably broader, as expected from the model studies [13]. In addition, as was first noted in the previous shape investigation [15], the steep gradient region is actually broader in the double-null shape; accordingly, the total pedestal pressure is enhanced for the same maximum gradient. This result is illustrated in Fig. 7. The improved pedestal pressure also leads to an improvement in global confinement. By adjusting the rotation as is shown in Fig. 2, we have produced confinement improvements up to 35% relative to the same plasmas with lower rotation speeds; an example of the associated changes in the radial profiles is given in Fig. 8. Furthermore, we have used edge rotation control to produce pedestal densities up to one-half the Greenwald density [9] in some shots.

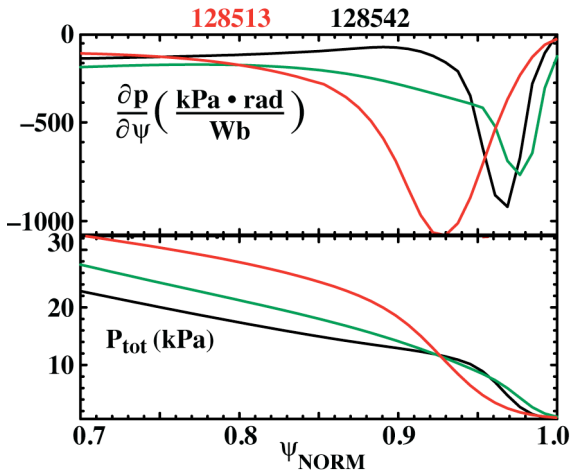

FIG. 7. Edge radial profiles of total pedestal pressure and edge pressure gradient for a double-null discharge (128513) and for two times in a single-null discharge (128542) showing broader region of steep edge gradient for the double null plasmas. The radial coordinate is the poloidal flux function normalized to one at the separatrix.

One of the long term goals of fusion research has been to develop techniques to control transport in the plasma. One conventionally thinks of this in terms of techniques for transport reduction. However, in the edge of a conventional H-mode, transport is already too small, since the heat and particle fluxes drive the edge pressure gradient into the ELMing stability

limit. The key to ELM-free operation is to increase transport enough so that the transport-limited edge gradients remain in the peeling-ballooning stable region. However, the edge gradients need to be as high as possible to optimize global confinement. The present QH-mode results demonstrate one transport control technique which uses variation in the edge rotation to continuously adjust the edge particle transport.

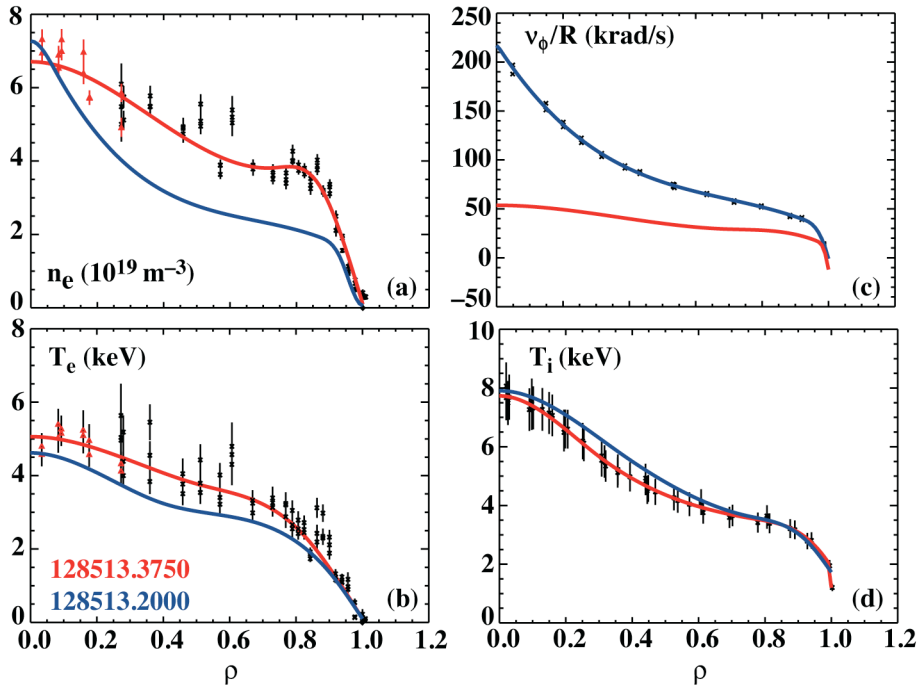

FIG. 8. Radial profiles showing change in radial profiles as input torque is changed. (a) Electron density, (b) electron temperature, (c) toroidal angular rotation speed, and (d) ion temperature. Positive angular rotation speed values correspond to counter rotation. Radial coordinate is proportional to the square root of the toroidal flux, normalized to unity at the separatrix.

4. QH-mode with Strong Edge Co-rotation

All previous QH-mode plasmas have exhibited edge rotation in the counter direction [1–8]. As is shown in Fig. 3, we have now created QH-mode plasmas with strong edge co-rotation in discharges with 100% co-injection. Figure 3 shows that these shots have all the usual QH-mode features: (1) ELM-free operation with constant density and radiated power, (2) H-mode level of confinement including the usual H-mode edge pedestal, and (3) enhanced edge particle transport due to the EHO. The operational recipe for these plasmas is quite similar to that used for QH-modes with counter injection. Low density operation using divertor cryopumping was one key factor. A second technique employed was feedback control of the neutral beam power to hold normalized beta β_N constant at 1.7 after the L-to-H transition; this produces the neutral beam power waveform shown in Fig. 3. Operationally, this recipe produced large toroidal rotation speeds in the edge pedestal of up to 200 km/s. As can be seen in Fig. 9, magnitude of the rotation speed is approximately twice that seen in counter injected QH-mode plasmas of similar shape and with similar torque input.

From the standpoint of comparing with theory, the magnitude of the edge rotation shear is more important than the magnitude of the rotation itself. As can be seen in Fig. 9, the magnitude of this shear is similar for both the co and counter NBI cases during the QH-mode phases. This is consistent with the theory of the EHO discussed earlier [13]. Also shown in Fig. 9 is a comparison shot with zero net input torque produced by using balanced beam injection. As can be seen there, the magnitude of the edge rotational shear is significantly lower in this case. There is no EHO in this shot; the rotation measurement is from a time

when the plasma is in the standard ELM-free state. The absence of the EHO in this case with low rotation shear is also consistent with the theory [13].

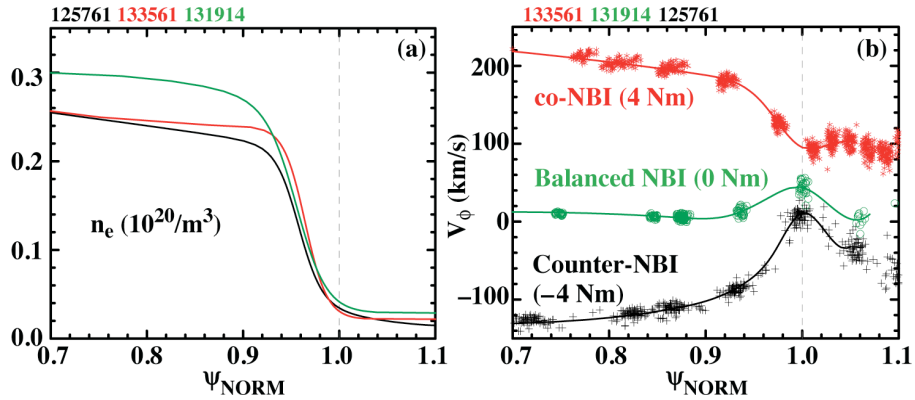

FIG. 9. Edge rotation shear comparison of co, counter and balanced NBI shots with similar input power (4–5 MW) and input torque (4 Nm). The co and counter shots are QH-mode, the balanced beam shot is a standard, ELM-free H-mode at the time shown. (a) Edge density, (b) edge toroidal rotation profile. Rotation is positive in the co-direction. Radial coordinate is the poloidal flux function normalized to one at the separatrix. Note that the pedestal densities are similar in the three cases; accordingly, the rotation differences are not due to differences in the edge density.

At present, co-NBI QH-modes lasting up to about 1 s have been seen on DIII-D. The termination of the QH-mode may be due to the decay of the edge rotation shear. As can be seen in Fig. 3(f), the pedestal rotation decreases and the separatrix rotation increases slowly with time during the QH-mode phase. The power level used in the QH-mode phase of these discharges (< 4 MW) is low when compared to that usually used in counter-NBI QH-modes, such as those in Figs. 1 and 2. It may be that the input torque in the present experiments was somewhat too low for fully sustained QH-mode operation. In the future, co-NBI QH-modes with higher input power and torque will be investigated.

The first co-rotating QH-mode seen on DIII-D was discovered serendipitously during an experiment run for another purpose. Given the advantages of double-null plasma shaping, it was somewhat surprising that this occurred in a lower single-null divertor shape. The results reported here come from a dedicated experiment which began from that serendipitous operating point. As can be seen in Fig. 10, these co-rotating QH-modes also operate near the peeling stability boundary. This lower single-null shape actually has reasonably good edge stability properties, exhibiting a normalized edge p' value significantly above those seen in Figs. 4 and 6, for example. The width of the steep gradient region, however, is more comparable to the single-null cases shown in Fig. 7.

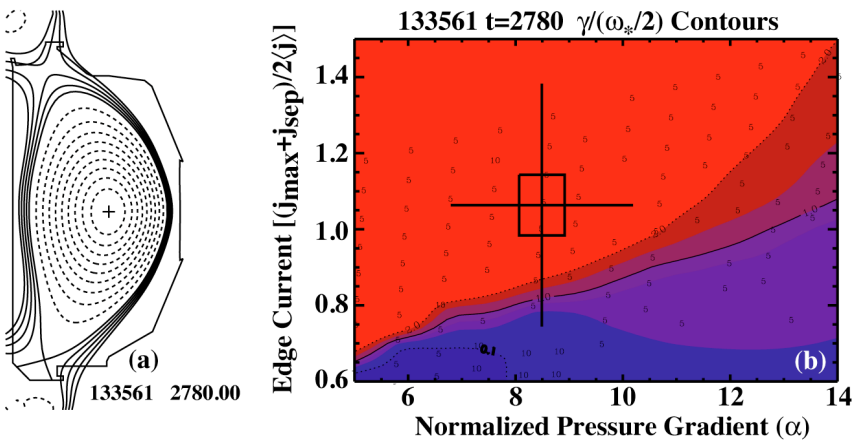

Fig. 10. (a) plasma shape, (b) and peeling-ballooning stability diagram for co-rotating QH-mode. Within the error bar, the operating point shown in (b) is on the stability boundary.

5. Conclusions

During the past two years, we made two significant discoveries about the QH-mode. First, we found that we can control the edge pedestal density and pressure by altering the edge particle transport through changes in the edge toroidal rotation. This allows us to adjust the edge operating point to be close to, but below the ELM stability boundary. This boundary is higher in more strongly shaped plasmas, which broadens the operating space available for QH-mode and leads to improved core performance. Second, for the first time on any tokamak, we have created QH-mode plasmas with strong edge co-rotation. This result demonstrates that counter NBI and counter edge rotation are not essential conditions for QH-mode. Both these investigations benefited from the edge stability predictions based on peeling-ballooning mode theory. That theory has been extended to provide a theory for the EHO [13]. Many of the features of that theory agree with the experimental results reported either previously [12] or in the present paper. One notable example is the prediction that co-rotating QH-mode is possible provided sufficient shear in the edge rotation can be created.

Acknowledgments

This work supported by the US Department of Energy under DE-FC02-04ER54698, DE-AC52-07NA27344 and DE-AC02-76CH03073.

References

[1] BURRELL, K.H., et al., Phys. Plasmas **12**, 056121 (2005).
[2] BURRELL, K.H., et al., Bull. Am. Phys. Soc. **44**, 127 (1999).
[3] BURRELL, K.H., et al., Phys. Plasmas **8**, 2153 (2001).
[4] SUTTROP, W., et al., Plasma Phys. Control. Fusion **45**, 1399 (2003).
[5] SUTTROP, W., et al., Nucl. Fusion **45**, 721 (2005).
[6] SAKAMOTO, Y., et al., Plasma Phys. Control. Fusion **46**, A299 (2004).
[7] OYAMA, N., et al., Nucl. Fusion **45**, 871 (2005).
[8] WEST, W.P., et al., Nucl. Fusion **45**, 1708 (2005).
[9] GREENWALD, M., et al., Nucl. Fusion **28**, 2199 (1988).
[10] SNYDER, P.B., et al., Nucl. Fusion **44**, 320 (2004).
[11] SNYDER, P.B., et al., Phys. Plasmas **12**, 056115 (2005).
[12] OSBORNE, T.H., et al., J. Physics: Conference Series **123**, 012014 (2008).
[13] SNYDER, P.B. ,et al., Nucl. Fusion **47**, 961 (2007).
[14] SCOVILLE, J.T., Fusion Sci. Technol. **52**, 398 (2007).
[15] LEONARD, A.W., et al., Nucl. Fusion **47**, 552 (2007).